

## Comparison of Nonlinear Dynamics of Parkinsonian and Essential Tremor

Olga E. Dick

Pavlov Institute of Physiology of Russian Academy of Science, nab. Makarova 6,  
199034, St. Petersburg, Russia  
(E-mail: [glazov.holo@mail.ioffe.ru](mailto:glazov.holo@mail.ioffe.ru))

**Abstract.** It is known that wrong clinical diagnosis of Parkinson's disease is about 20 % among patients suffering from pathological tremor. That is why the search of new possibilities to improve the diagnostics has high priority. The aim of the work is to answer the question whether the methods of nonlinear dynamics can be used for the guaranteed differential diagnostics of two main types of pathological tremor (parkinsonian and essential ones). We have analyzed tremor determined as fast involuntary shaking and arising during the performance of the motor task by healthy subjects and two groups of patients with parkinsonian syndrome. The first group has the primary Parkinson's disease and the second group has the essential tremor as finger's shaking during the some movements as the main symptom. Using the wavelet transform modulus maxima method, the calculation of the Hölder exponents as well as the detection of unstable periodic orbits and surrogate data we demonstrate the statistically confirmed differences in dynamical complexity, multifractality degree and number of unstable periodic orbits for the two groups of patients. The results give the positive answer the question rose in the work.

**Keywords:** Dynamical Complexity, Unstable Periodic Orbits, Multifractality, Parkinson's disease, Essential Tremor.

### 1 Introduction

In spite of enormous number of works [1, 2] devoted to the study of pathological tremor the topic is of immediate interest because of large number of clinical errors connected with wrong administration of antiparkinsonian drugs for subjects having tremor symptoms but not having Parkinson's disease. For example, parkinsonian tremor and so called essential tremor (or action tremor) when the body parts are involved into involuntary shaking during the movement performance differ by frequency. The frequency in essential tremor, however, declines with age in the side of the parkinsonian tremor frequency [3] so that oldest patients can be objects of clinical errors.

The aim of the work is to answer the question whether the methods of nonlinear dynamics can be used for the guaranteed differential diagnostics of two main types of pathological tremor (parkinsonian and essential ones).

Received: 2 April 2015 / Accepted: 5 October 2015

© 2015 CMSIM



ISSN 2241-0503

We studied involuntary shaking (tremor) of fingers accompanied the performance of the motor task such as sustaining the given effort of human hands under isometric conditions (without finger movement in space). For estimating the tremor features we used the methods of nonlinear dynamics such as the wavelet transform and multifractal analysis as well as recurrence plot technique for detecting unstable periodic orbits and surrogate data. We demonstrate the use of these methods for a diagnostics of the human motor dysfunction.

## 2 The experimental procedure

We used the results of testing 10 healthy subjects aged 47-54 years, 6 parkinsonian patients with bilateral akinesia and tremor aged 45-62 years and 7 subjects with syndrome of essential tremor and without other symptoms of Parkinson's disease. The motor task was to control the isometric muscle effort with the strength of muscle contraction shown by the positions of marks on a monitor. The subjects sat in front of a monitor standing on a table and pressed on platforms containing stress sensors with their fingers. The sensors transformed the pressure strength of the fingers of each hand into an electric signal. The rigidity of the platforms made it possible to record the effort in the isometric mode, i.e., without noticeable movement of fingers at the points of contact with the sensors. The isometric effort was recorded for 50 s. The subject's fingers sustained an upward muscle effort, with the back of each hand pressing against the base of the platform.

The patients with Parkinson's disease did not take any drugs before the test on the day of testing. Usually, these patients received levodopa, an antiparkinsonian preparation three times a day to compensate for dopamine deficiency. The subjects with syndrome of essential tremor did not have tremor medication.

The recorded trajectory of isometric effort consisted of a slow trend and a fast involuntary component (tremor), which was isolated from the recorded trajectory using the MATLAB software.

## 3 Wavelet transform and multifractality

### 3.1 Estimation the global wavelet spectrum of the tremor

To evaluate the difference between physiological and pathological tremors, we used the wavelet transform modulus maxima (WTMM) method [4] based on the continuous wavelet transform of a time series describing the examined tremor  $x(t)$ :

$$W(a, t_0) = a^{-1/2} \int_{-\infty}^{+\infty} x(t) \psi^* \left( (t - t_0) / a \right) dt,$$

where  $a$  and  $t_0$  are the scale and space parameters,  $\psi((t-t_0)/a)$  is the wavelet function obtained from the basic wavelet  $\psi(t)$  by scaling and shifting along the time, symbol  $*$  means the complex conjugate. As the basic wavelet we use the complex Morlet wavelet:

$$\psi_0(t) = \pi^{-1/4} \exp(-0.5t^2) (\exp(i\omega_0 t) - \exp(-0.5\omega_0^2)),$$

where the second component in brackets can be neglected at  $\omega_0=2\pi>0$ , the multiplier factor  $\exp(i\omega_0 t)$  is a complex form of a harmonic function modulated by the Gaussian  $\exp(-0.5t^2)$ , the coefficient  $\pi^{-1/4}$  is necessary to normalize the wavelet energy. The value  $\omega_0=2\pi$  gives the simple relation  $f=1/a$  between the scale  $a$  and the frequency  $f$  of the Fourier spectrum. Then expression has the form:

$$W(f, t_0) = \pi^{-1/4} \sqrt{f} \int_{-\infty}^{+\infty} x(t) \exp(-0.5(t-t_0)^2 f^2) \exp(-i2\pi(t-t_0)f) dt.$$

The modulus of the wavelet spectrum  $|W(f, t_0)|$  characterizes the presence and intensity of the frequency  $f$  at the moment  $t_0$  in the signal and  $|W(f, t_0)|^2$  describes the instantaneous distribution of the tremor energy over frequencies, that is, the local spectrum of the signal energy at the time  $t_0$ .

The value

$$E(f) = \int_{t_1}^{t_2} |W(f, t_0)|^2 dt_0$$

determines the global wavelet spectrum, i.e., the integral distribution of the wavelet spectrum energy over frequency range on the time interval  $[t_1, t_2]$ .

### 3.2 Estimation the tremor multifractality

Information about possible multifractal feature of the signal and its localization  $t_0$  reflects in the asymptotic behavior of coefficients  $|W(a, t_0)|$  at small  $a$  values and large  $f$  values, respectively. Abnormal small decrease of the wavelet coefficients at  $a \rightarrow 0$  in a neighborhood of the point  $t_0$  testifies about singularity of the signal at the point. Thus, the rate of the change of the modulus of the wavelet coefficients enables to analyze the presence or absence of singularities of the signal.

The degree of singularity of the signal  $x(t)$  at the point  $t_0$  is described by the Hölder exponent,  $h(t_0)$ , the largest exponent such that the analyzed signal in a neighborhood of the point  $t_0$  can be represented as the sum of the regular component (a polynomial  $P_n(t)$  of order  $n < h(t_0)$ ) and a member describing a non - regular behavior [4]:

$$x(t) = P_n(t) + c|t-t_0|^{h(t_0)}.$$

The value  $h(t_0)$  is the measure of singularity of the signal at the point  $t_0$  since

the smaller  $h(t_0)$  value, the more singular the signal. The Hölder exponents characterize the presence of correlations of different types in the analyzed process, e.g., anti-correlated ( $h < 0.5$ ) or correlated ( $h > 0.5$ ) dynamics or absence of correlations ( $h = 0.5$ ).

The Hölder exponents are found on the basis of statistical description of local singularities by partition functions [5]. The algorithm consists of the following procedures.

- 1) The continuous wavelet transform of the time series is used.
- 2) A set  $L(a)$  of lines of local modulus maxima of the wavelet coefficients is found at each scale  $a$
- 3) The partition functions are calculated by the sum of  $q$  powers of the modulus maxima of the wavelet coefficients along the each line at the scales smaller the given value  $a$ :

$$Z(q, a) = \sum_{l \in L(a)} \left( \sup_{a' \leq a} |W(a', t_l(a'))| \right)^q,$$

$t_l(a^*)$  determines the position of the maximum corresponding to the line  $l$  at this scale

- 4) The partition function is  $Z(q, a) \sim a^{\tau(q)}$  at  $a \rightarrow 0$  [5], therefore, the scaling exponent can be extracted as

$$\tau(q) \sim \log_{10} Z(q, a) / \log_{10} a.$$

- 5) Choosing different values of the power  $q$  one can obtain a linear dependence  $\tau(q)$  with a constant value of the Hölder exponent

$$h(q) = d\tau(q)/dq = \text{const}$$

for monofractal signals and nonlinear dependence  $\tau(q) = qh(q) - D(h)$  with large number of the Hölder exponents for multifractal signals.

- 6) The singularity spectrum (distribution of the local Hölder exponents) is calculated from the Legendre transform [5]:

$$D(h) = qh(q) - \tau(q).$$

Using the global wavelet spectra and the WWTM algorithm for the different tremor recordings we obtain the maximum of the global tremor energy ( $E_{\max}$ ) and two multifractal parameters: a) the width of the singularity spectrum

$$\Delta h = h_{\max} - h_{\min},$$

where  $h_{\max}$  and  $h_{\min}$  are the maximal and minimal values of the Hölder exponent corresponding to minimal and maximal tremor fluctuation, respectively; b) the asymmetry of the singularity spectrum

$$\Delta = |\Delta_2 - \Delta_1|,$$

where  $\Delta_1 = h_{\max} - h_0$  and  $\Delta_2 = h_0 - h_{\min}$ ,  $h_0 = h(q = 0)$ .

Smaller  $\Delta h$  indicates that the time series tends to be monofractal and larger  $\Delta h$  testifies the enhancement of multifractality. The asymmetry parameter  $\Delta$  characterizes where, in the region of strong singularities ( $q > 0$ ) or in the region of weak singularities ( $q < 0$ ), the singularity spectrum is more concentrated.

To compare the mean values in each of the examined group of subjects the Student criterion was applied.

#### 4 Recurrence plot and localization of unstable periodic orbits

The set of unstable periodic orbits (UPOs) which form the skeleton of the chaotic attractor can be found by the recurrence quantification analysis (RQA) [6]. The calculation for the RQA was performed using the CRP Toolbox, available at [tocsy.pik-potsdam.de/crp.php](http://tocsy.pik-potsdam.de/crp.php).

A recurrence plot (RP) is a graphical representation of a matrix defined as

$$R_{i,j}(m, \varepsilon) = \Theta(\varepsilon - \|y_i - y_j\|),$$

where  $\varepsilon$  is an error (threshold distance for RP computation),  $\Theta(\cdot)$  is the Heaviside function, symbol  $\|\cdot\|$  denotes a norm and  $y$  is a phase space trajectory in a  $m$ -dimension phase space [7]. The trajectory can be reconstructed from a time series by using the delay coordinate embedding method [8].

The values  $R_{i,j} = 1$  and  $R_{i,j} = 0$  are plotted as gray and white dots, reflecting events that are termed as recurrence and nonrecurrence, respectively.

The recurrence time is defined as the time needed for a trajectory of a dynamical system to return into a previously visited neighborhood [9].

The pattern corresponding to periodic oscillations (periodic orbits) is reflected in the RP by noninterrupted equally spaced diagonal lines. The vertical distance between these lines corresponds to the period of the oscillations. The chaotic pattern leads to the emergence of diagonals which are seemingly shorter. The vertical distances become irregular. When the trajectory of the system comes close to an unstable periodic orbit (UPO), it stays in its vicinity for a certain time interval, whose length depends on how unstable the UPO is [9, 10]. Hence, UPOs can be localized by identifying such windows inside the RP, where the patterns correspond to a periodic movement. If the distance between the diagonal lines varies from one chosen window to the other then various UPOs coexist with different periods.

The period of UPO can be estimated by the vertical distances between the recurrence points in the periodic window multiplied by the sampling time of the data series [9, 11].

The algorithm for finding UPOs consists of the following procedures.

1. A phase space trajectory  $y(t)$  is reconstructed from a measured time series  $\{x(t)\}$  by the delay coordinate embedding method:

$$y(t) = (x(t), x(t+d), \dots, x(t+(m-1)d),$$

where  $m$  is the embedding dimension and  $d$  is the delay time. Parameters  $m=5$  and  $d=2$  were chosen on the basis of first minimum of the mutual information function and the false nearest neighbor method [12].

2. To identify unstable periodic orbits a recurrence plot

$$R_{i,j}(m, \varepsilon) = \Theta(\varepsilon - \|y_i - y_j\|),$$

is constructed with the threshold distance  $\varepsilon$  equal to 1% of the standard deviation of the data series.

3. The recurrence times of second type [10] are found for the recurrence neighbourhood of radius  $\epsilon$ . The values of recurrence periods are determined as recurrence times multiplied by the sampling time of the data series. The values are recorded in a histogram. The periods of UPOs are the maxima of the histogram of the recurrence periods.

4. To exclude the noise influence the obtained UPOs are tested for statistical accuracy. For this purpose the procedure is repeated for 30 surrogates obtained as randomized versions of the original data. In the surrogate data the time interval sequences are destroyed by randomly shuffling the locations of the time intervals of original data [13].

The statistical measure of the presence of statistically significant UPOs in the original time series is given by the ratio

$$k = (A - \bar{A}) / \sigma,$$

where  $A$  is the value of maximum of the histogram,  $\bar{A}$  is the mean of  $A$  for surrogates and  $\sigma$  is a standard deviation. The value of  $k$  characterizes the existence of statistically significant UPOs in the original data in comparison with its surrogate (noisy) version. The value  $k > 2$  means the detection of UPOs with a greater than 95% confidence level.

## 5 Results and discussion

Examples of fast component of the isometric force trajectory of the human hand (tremor) for the healthy subject, the patient with Parkinson disease and for the subject with essential tremor as well as their global wavelet spectra are given in Fig.1. The healthy and pathological tremors differ by spectra maxima. The maximum ( $E_{\max}$ ) of the physiological tremor spectrum is in the frequency range of the alpha rhythm [8, 14] Hz. For the pathological tremor  $E_{\max}$  is shifted in the theta range [4, 7.5] Hz and it increases in ten times in the parkinsonian tremor and in five times in the essential one as compared with the healthy tremor. The essential tremor spectrum has two peaks as opposed to the parkinsonian tremor but the values of the peaks do not differ significantly.

Figure 2 illustrates the differences in the singularity spectra  $D(h)$  for the same subjects. The form of spectrum testifies the multifractality of both physiological and parkinsonian tremor but the spectra differ for the three examples.

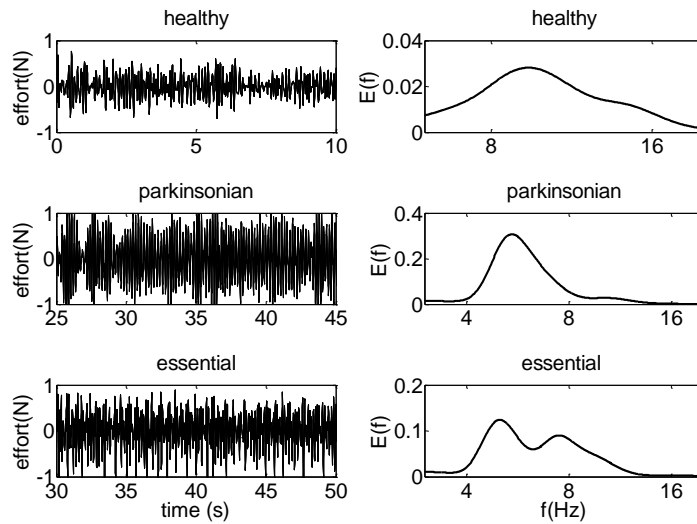


Fig.1 Examples of healthy, parkinsonian and essential tremors (left column) and their global wavelet spectra  $E(f)$  (right column)

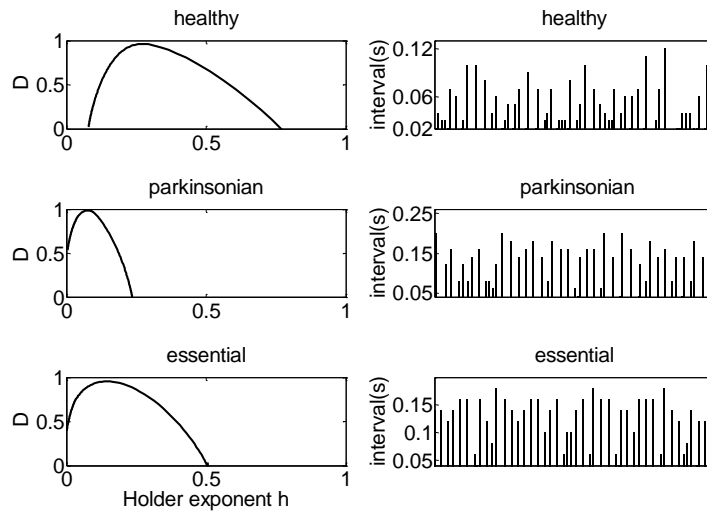


Fig. 2 Examples of the singularity spectra  $D(h)$  for the different tremors (left column) and intervals between local maxima of the tremor data (right column)

The healthy tremor is characterized by the largest width  $\Delta h$  of the singularity spectrum and, therefore, by the significant degree of multifractality. The decline in the width of the spectrum shows a fall in the multifractality degree. It means a reduction of nonuniformity of the pathological tremors. We illustrate it in the right column of Figure 2 where intervals between local maxima of the tremor data are depicted.

The parkinsonian tremor is characterized by the smallest width of the singularity spectrum and its smallest asymmetry ( $\Delta$ ). The values of  $\Delta h$  and  $\Delta$  for the essential tremor are larger than for the parkinsonian one but they do not exceed the values for healthy tremor.

The decrease of the both parameters in pathological tremor is due to decreasing contribution of weak fluctuations (for  $q < 0$ ). These fluctuations lead to the expansion of the singularity spectrum and emergence of both anticorrelated (for  $h < 0.5$ ) and correlated (for  $h > 0.5$ ) dynamics of sequent intervals between local maxima of the tremor data.

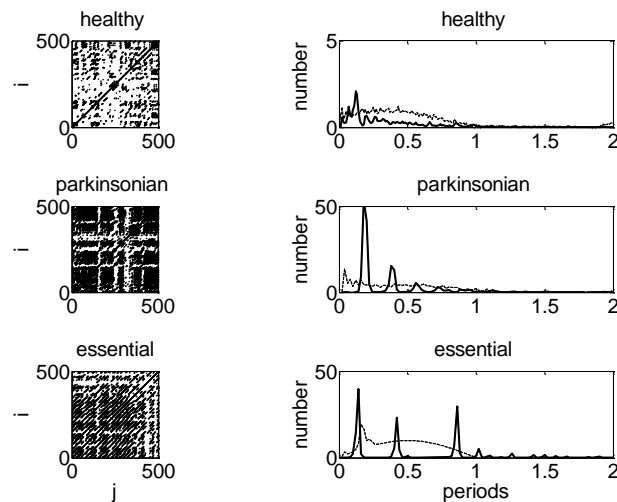


Fig. 3. Examples of recurrence plots for the different tremors (left column) and histograms of recurrence periods for tremor data and their surrogates (right column, solid and dash-and-dot lines, respectively).

Parameters: the embedding dimension  $m=5$ , the delay time  $d=2$ , the threshold distance  $\varepsilon=1\%$  of the standard deviation of the data series.

The recurrence plots depicted in Figure 3 exhibit non-homogeneous but quasi-periodic recurrent structures reflecting in that the distances between the diagonal lines vary in all the three considered tremors. The RP of the healthy tremor is characterized by small black rectangles, whereas the RPs from the pathological tremors show larger rectangles. These rectangles may reflect time intervals when the trajectory is travelling near the corresponding UPOs [10].

The recurrence times obtained from the RP given in the Figure 3 are clustered in the intervals around the value  $i=24$  for the healthy tremor, around  $i=36$  and  $72$

for the parkinsonian one and around  $i=28, 84$  and  $168$  for the essential tremor. Taking into account the value of the sampling rate value  $dt=0.005(s)$  the recurrence periods are equal to  $0.12 (s)$  for the healthy data,  $0.18 (s)$  and  $0.36 (s)$  for the parkinsonian data and  $0.14 (s)$ ,  $0.42 (s)$  and  $0.84 (s)$  for the essential data. These recurrence periods were extracted as peaks of the histograms given in the right column of Figure 3 (solid lines). The periods obtained can be used for localization of UPOs.

Testing surrogate data we excluded the values  $0.12 (s)$  and  $0.36 (s)$  since the statistical measure  $k < 1$  in both cases. For other recurrence periods extracted from Figure 3 the value  $k > 2$  that supports the detection of UPOs with a greater than 95% confidence level. Thus, for the healthy tremor data represented in Figure 3 there are no statistically significant UPOs. By contrast, the UPO of period 1 ( $0,18 s$ ) is found for the parkinsonian tremor and the UPOs of periods 1, 3 and 6 are obtained for the essential tremor ( $0.42/0.14=3, 0.84/0.14=6$ ).

The similar dynamics of the wavelet and multifractal parameters as well as UPOs localization is observed for all the examined subjects. It enables us to use the common practice of averaging the recordings of all subjects for testing significant variations among the groups.

The values of  $E_{max}$ ,  $\Delta h$ ,  $\Delta$  and statistical measures  $k$  for UPOs of various periods averaged by subjects in every group are given in Table 1.

| tremor     | hand  | healthy           | parkinsonian    | essential       |
|------------|-------|-------------------|-----------------|-----------------|
| $E_{max}$  | left  | $0.029 \pm 0.001$ | $0.45 \pm 0.02$ | $0.25 \pm 0.01$ |
|            | right | $0.037 \pm 0.003$ | $0.56 \pm 0.04$ | $0.31 \pm 0.02$ |
| $\Delta h$ | left  | $0.83 \pm 0.08$   | $0.22 \pm 0.02$ | $0.49 \pm 0.05$ |
|            | right | $0.76 \pm 0.09$   | $0.27 \pm 0.02$ | $0.42 \pm 0.04$ |
| $\Delta$   | left  | $0.46 \pm 0.04$   | $0.09 \pm 0.01$ | $0.27 \pm 0.03$ |
|            | right | $0.38 \pm 0.03$   | $0.12 \pm 0.01$ | $0.20 \pm 0.02$ |
| $k(p_1)$   | left  | $<1$              | $4.9 \pm 0.8$   | $5.7 \pm 0.9$   |
|            | right | $<1$              | $3.8 \pm 0.6$   | $4.5 \pm 0.8$   |
| $k(p_2)$   | left  | $<1$              | $<1$            | $<1$            |
|            | right | $<1$              | $2.1 \pm 0.6$   | $<1$            |
| $k(p_3)$   | left  | $<1$              | $<1$            | $2.1 \pm 0.3$   |
|            | right | $<1$              | $<1$            | $2.7 \pm 0.3$   |
| $k(p_6)$   | left  | $<1$              | $<1$            | $3.8 \pm 0.4$   |
|            | right | $<1$              | $<1$            | $4.1 \pm 0.4$   |

Table 1. Comparison of the mean values of wavelet and singularity spectra characteristics and statistical measure of UPOs (averaging over subjects inside the every examined group).

The significant distinctions between the states (pathological or physiological tremor) are identified by all the parameters ( $p < 0.03$ ). The values for the essential and parkinsonian tremors also differ ( $p < 0.05$ ).

The results serve one more verification for the decline of dynamical complexity of time intervals in pathological tremor. It exhibits in the decrease of the

multifractality degree, disappearance of long-range correlations and transitions to strongly periodic dynamics including the emergence of unstable periodic orbits in involuntary oscillations of the human hand.

## Conclusions

Our study of differences in involuntary oscillations arising during the maintenance of isometric force by the human hand of a subject suffering from Parkinson' disease and a subject having tremor symptoms but not having the disease demonstrates that the multifractal characteristics and number of UPOs can serve useful indicators of a dysfunctional network in the central nervous system.

## References

1. J. H. McAuley, C. D. Marsden. Physiological and pathological tremors and rhythmic central motor control. *Brain*, 123, 8, 1545{1567, 2000.
2. A.N. Pavlov, A.N. Tupitsyn, A. Legros, et. al. Using wavelet analysis to detect the influence of low frequency magnetic fields on human physiological tremor, *Physiol. Measurement*, 28, 321{333, 2007.
3. R. J. Elble, C. Higgins, K. Leffler et, al. Factors influencing the amplitude and frequency of essential tremor. *Mov. Disord.*, 9, 589{596, 1994.
4. J. F. Muzy, E. Bacry, A. Arneodo. Multifractal formalism for fractal signals: the structure-function approach versus the wavelet-transform modulus-maxima method. *Phys. Rev. E*, 47, 875{884, 1993.
5. A. Arneodo, E. Bacry, J. F Muzy. The thermodynamics of fractals revisited with wavelets. *Physica A*, 213, 232{275, 1995.
6. J. P. Eckmann, S. Kamphorst, D. Ruelle. Recurrence plots of dynamical systems. *Europhys. Lett.*, 4, 973{977, 1987.
7. N. Marwan, M. C. Romano, M. Thiel, et. al. Recurrence plots for the analysis of complex systems. *Physics Reports*, 438, 237{329, 2007.
8. F. Takens. Detecting strange attractors in turbulence, *Dynamical Systems and Turbulence*, Lecture Notes in Mathematics ( D. Rand, L. S. Young, eds.), Springer-Verlag, Berlin 898, 366{381, 1981
9. J. B. Gao. Recurrence time statistics for chaotic systems and their applications. *Phys. Rev. Lett.*, 83, 16, 3178{3181, 1999.
10. E. Bradley, R. Mantilla. Recurrence plots and unstable periodic orbits. *Chaos*, 12, 3, 596{600, 2002.
- 11 E. J. Ngamga, A. Nandi, R. Ramaswamy, et. al., *Phys. Rev. E*, 75, 3 036222{036345, 2007.
12. M. B. Kennel, R. Brown, H. D. Abarbanel. Determining embedding dimension for phase-space reconstruction using a geometrical construction. *Phys. Rev. A*, 45, 6, 3403{3411, 1992.
13. J. Theiler, S. Eubank, A. Longtin, et, al. Testing for nonlinearity in time series: the method of surrogate data. *Physica D*, 58, 77{94, 1992.